Optimal tuning of lasing modes through collective particle resonance

Jorge Ripoll

Institute of Electronic Structure and Laser, Foundation for Research and Technology—Hellas, P.O. Box 1527, 71110 Heraklion, Crete, Greece

Costas M. Soukoulis

Institute of Electronic Structure and Laser, Foundation for Research and Technology—Hellas, P.O. Box 1527, 71110 Heraklion, Crete, Greece, and Ames Laboratory, U. S. Department of Energy, and Department of Physics and Astronomy, Iowa State University, Ames, Iowa 50011

Eleftherios N. Economou

Institute of Electronic Structure and Laser, Foundation for Research and Technology—Hellas, P.O. Box 1527, 71110 Heraklion, Crete, Greece

Received June 6, 2003; revised manuscript received July 22, 2003; accepted July 25, 2003

One of the current challenges in laser optics is to take advantage of the resonant modes within particles to obtain high-quality microcavities with low threshold. We present a study of the effect that the internal resonances of individual particles have on the emitted intensity, and demonstrate how optimal tuning of the size and separation of the particles can enhance the quality factor by more than four orders of magnitude. The potential applications of this work on the design of an optimal microcavity and on a random laser are discussed. © 2004 Optical Society of America

OCIS codes: 290.4210, 160.2540, 160.0160.

1. INTRODUCTION

The optimization of laser cavities that allow high-Q cavity modes has been an active field of research since the development of the laser.[1] In particular, the development of ultrahigh-Q, ultralow-threshold lasers is one of the key issues in the contemporary optical physics and quantum electronics community, with applications ranging from frequency stabilization of semiconductor diode lasers to environmental sensing by trace absorption detection in compact, integrated structures.[2] Of particular interest are small optical resonators that use microspheres[3–6] and microcylinders[7,8] as laser gain media since it has been shown that in some cases they present Q values as high as 10^{10}.[5,9]

Other more complex cavities have been explored, such as periodic lattices in one or two dimensions that sustain three-dimensionally bound modes of the radiation field.[10] However, all these high-Q cavities are based on geometries that present high symmetries. Lately, a novel approach to laser cavities has appeared that takes advantage of randomness in the system. These are based on novel materials that have been termed random lasers,[11,12] and that exhibit light amplification as a result of laser pumping of a gain medium in a strongly scattering environment. In these cases it is the multiple scattering that acts as a laser cavity[12–15] when gain exceeds losses.[15–17] Within such random media with gain, distinct lasing modes have been measured,[18–20] and coherence of the emitted light has been observed.[21] In theoretical studies it has been shown[22,23] that the emission peaks correspond to modes in the random system,[24] and that these may be selectively excited.[23] So far, the numerical methods that have been utilized to model light amplification in systems with complex geometries have been based on finite-difference-time-domain methods[22,23] and the dipolar approximation.[25] A common approximation that models the incoherent contribution of the emission spectrum is the diffusion approximation,[15,26] which is very convenient because most of the equations involved have an analytical solution.

Our approach to increasing the Q factor in microcavities is to make use of the interaction between particles to excite a collective resonance. Collective resonances occur when the multiple scattering between the particles is such that a resonance may be excited in both scatterers. Similar effects have been studied for dielectric particles on substrates[27,28] that form the basis of photonic-force microscopy.[29,30] We here present a theoretical study of the effect that collective particle resonances have on the Q factor of cylindrical scatterers with gain. We study this effect for two and three cylinders and show how the Q factor increases in some cases by four orders of magnitude in the presence of a collective resonance when compared with the case of isolated scatterers. To obtain accurate numerical results, we rigorously solve the scattering integral equations by using a two-dimensional (2-D) method that is applicable to any geometry.[31,32] Even though the study presented is for a small number of scatterers and is

 © 2004 Optical Society of America

thus closely related to microcavity lasers, we believe that the development of laser powders with controlled particle diameter such that the excitation of collective resonances is possible will significantly increase the Q factor in random lasers and lower their threshold.

This work is organized as follows: In Section 2 we present the scattering equations that model light propagation in a medium with a collection of M arbitrarily shaped scatterers. Gain is introduced among the scatterers through the resonance approximation for a collection of atoms.[1] In Section 3 we present results for an isolated cylinder, two cylinders, and three cylinders versus the population inversion and the wavelength. In Section 4 we discuss the implications of our findings.

2. SCATTERING EQUATIONS

We shall study the scattering cross section and the intensity distribution of a collection of scatterers with a complex dielectric constant induced through population inversion. For a material with dielectric constant ϵ_n, we will introduce gain by assuming a three-level laser, in which case the (now spatially dependent) dielectric constant may be modeled through the resonance approximation for a collection of atoms as[1]

$$\epsilon_{\text{laser}}(\mathbf{r}) = \epsilon_n\left[1 - \frac{3\lambda^3}{4\pi^2}\frac{\gamma_{\text{rad}}^{1\to 0}}{\Delta\omega_a^{1\to 0}}\Delta N_{01}(\mathbf{r})\Lambda(\omega,\ \omega_a^{1\to 0})\right], \tag{1}$$

where λ is the wavelength, $\gamma_{\text{rad}}^{1\to 0}$ is the decay rate from the excited level to the ground level in seconds, $\Delta\omega_a^{1\to 0}$ is the FWHM line width of the atomic transition from level 1 to the ground level, and $\Delta N_{01}(\mathbf{r}) = N_0(\mathbf{r}) - N_1(\mathbf{r})$ is the population difference between level 1 and the ground state, with $N_t \approx N_0(\mathbf{r}) + N_1(\mathbf{r})$ being the total electron density. We shall assume that $N_2 \ll N_0 + N_1$ because of the fast decay rate of level 2 to excited state level 1 ($\gamma_{\text{rad}}^{2\to 1} \gg \gamma_{\text{rad}}^{1\to 0}$). In Eq. (1) Λ is the Lorenztian line shape[1] for the laser transition:

$$\Lambda(\omega,\ \omega_a^{1\to 0}) = \left\{\frac{2(\omega - \omega_a^{1\to 0})/\Delta\omega_a^{1\to 0}}{1 + [2(\omega - \omega_a^{1\to 0})/\Delta\omega_a^{1\to 0}]^2} + i\frac{1}{1 + [2(\omega - \omega_a^{1\to 0})/\Delta\omega_a^{1\to 0}]^2}\right\}, \tag{2}$$

where $\omega = 2\pi c/\lambda$ is the frequency, c being the speed of light in vacuum, and $\omega_a^{1\to 0}$ is the frequency of the transition from level 1 to the ground state corresponding to a wavelength λ_{laser}. All calculations presented in this work were performed by choosing the values shown in Table 1 for the constants in Eqs. (1) and (2); these values, taken from Ref. 22, are based on real materials.[12] The behaviors of the complex dielectric constant and the index of refraction versus wavelength for different inversion populations N_1/N_t are shown in Fig. 1, where we have assumed a dielectric constant $\epsilon_n = 5.76$ in Eq. (1) corresponding to an index of refraction of $n_n = 2.4$.

Table 1. Optical Parameters Used in Eqs. (1) and (2) to Derive the Dielectric Constant in the Presence of Gain

Constant	Value	Constant	Value
ϵ_n	5.76	$\omega_a^{1\to 0}$	376,991 rad/ns
$n_n = \sqrt{\epsilon_n}$	2.4	$\Delta\omega_a^{1\to 0}$	94,000 rad/ns
N_t	3.311×10^{-3} nm^{-3}	λ_{laser}	500 nm
$\gamma_{\text{rad}}^{1\to 0}$	1 ns		

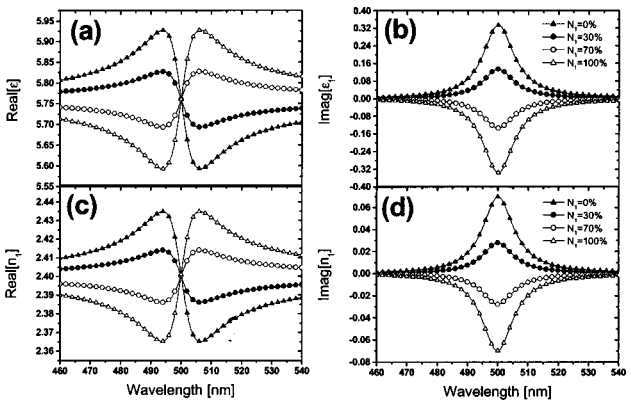

Fig. 1. Values of the dielectric constant and index of refraction inside the scatterers for $N_1/N_t = 0$, 30, 70, and 100%, for (a) real, (b) imaginary parts of the dielectric constant ϵ_1 and (c) real, (d) imaginary parts of the index of refraction n_1.

As seen from Eq. (1), the dielectric constant within the cylinders is spatially inhomogeneous because it depends nonlinearly on the pumping intensity and emitted field within the cylinder through ΔN_{01}.[1] Since we are interested in studying the changes in scattering cross section of a collection of scatterers with the (emitted) wavelength, we will not address the laser dynamics, and therefore will not solve the nonlinear problem self-consistently as was done in Refs. 22 and 23. To include the population inversion in Eq. (1), we will consider that the spatially dependent dielectric constant within each scatterer may be written as $\epsilon_{\text{laser}}(\mathbf{r}) = \epsilon_1 + \delta\epsilon_{\text{laser}}(\mathbf{r})$, where $\epsilon_1 = \langle\epsilon_{\text{laser}}(\mathbf{r})\rangle$ is the average dielectric constant within each cylinder and $\delta\epsilon_{\text{laser}}(\mathbf{r}) = \epsilon_{\text{laser}}(\mathbf{r}) - \langle\epsilon_{\text{laser}}(\mathbf{r})\rangle$ is the deviation from the average value. This expression for ϵ_{laser} implies that we consider average population differences $\overline{\Delta N}_{10} = \bar{N}_0 - \bar{N}_1$ where $\bar{N}_0$ and $\bar{N}_1$ are the electron density in the ground and excited states, respectively, averaged within the volumes of the scatterers. In the 2-D case where the scalar wave equation may be applied, the equations for the electric field in terms of ϵ_1 and $\delta\epsilon_{\text{laser}}$, and for an arbitrary scattering geometry of total volume V, are written as[33]

$$\nabla^2 E_0(\mathbf{r}) + \epsilon_0\frac{\omega^2}{c^2}E_0(\mathbf{r}) = 0 \qquad \mathbf{r} \notin V,$$

$$\nabla^2 E_1(\mathbf{r}) + \epsilon_1\frac{\omega^2}{c^2}E_1(\mathbf{r}) = \alpha E_{\text{pump}}(\mathbf{r}) - \delta\epsilon_{\text{laser}}(\mathbf{r})\frac{\omega^2}{c^2}E_1(\mathbf{r}) \qquad \mathbf{r} \in V, \tag{3}$$

where ϵ_0 is the background dielectric constant, c is the speed of light in vacuum, E_{pump} is the pump field, α is a constant with units of inverse area, and E_0 and E_1 are

the fields outside and inside the scatterer, respectively. At this point we shall make use of the findings reported in Ref. 34 where the authors prove that the main contribution to the scattered intensity from inhomogeneous spheres comes from the volume-averaged dielectric constant. Following Ref. 34 we may therefore neglect $\delta\epsilon_{\text{laser}}$ when compared with $\epsilon_1 = \langle \epsilon_{\text{laser}}(\mathbf{r}) \rangle$. (The implications of this approximation are under study and will be presented in a future paper.) Introducing this approximation into Eq. (3) and applying Green's theorem we find the following 2-D scattering integral equations for a collection of M scatterers of volume V_i defined by surface S_i:

$$E(\mathbf{r}) = -\sum_{i=1}^{M} \Phi_i^+(\mathbf{r}) \qquad \mathbf{r} \notin V_{i=1\ldots M},$$

$$E_i(\mathbf{r}) = E_{\text{pump}}(\mathbf{r}) + \Phi_i^-(\mathbf{r}) \qquad \mathbf{r} \in V_i, \tag{4}$$

where

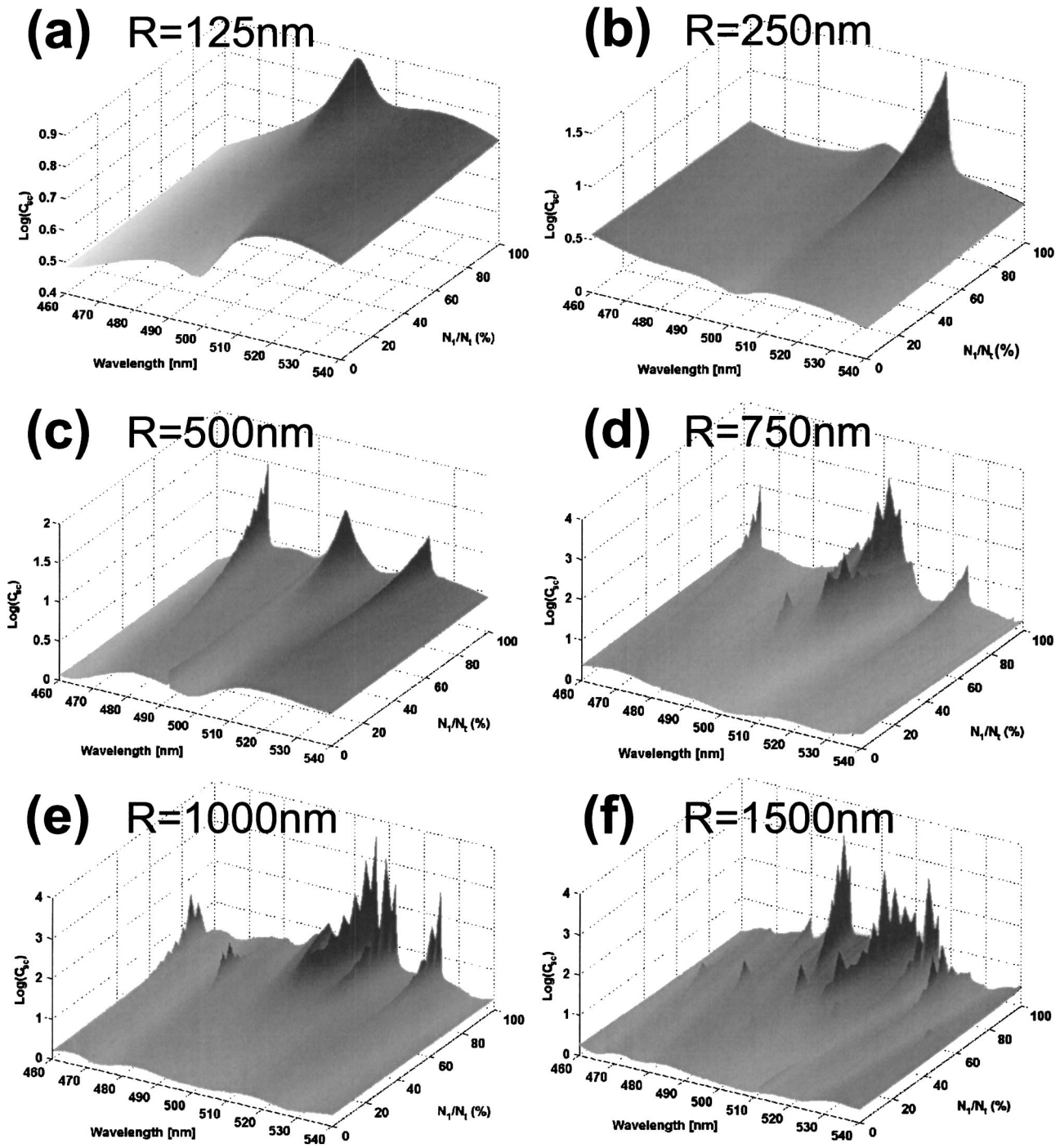

Fig. 2. Scattering cross section in log–scale for a single cylinder for *s* polarization versus population of the excited level N_1/N_t in % and wavelength in nm for R = (a) 125, (b) 250, (c) 500, (d) 750, (e) 1000, (f) 1500 nm.

$$\Phi_i^+(\mathbf{r}) = \frac{1}{4\pi}\int_{S_i}[\nabla G_0(\mathbf{r}-\mathbf{r}')E_i(\mathbf{r}') - G_0(\mathbf{r}-\mathbf{r}')\nabla E_i(\mathbf{r}')]\mathrm{d}\mathbf{S}' \qquad \mathbf{r}\notin V_i$$

$$\Phi_i^-(\mathbf{r}) = \frac{1}{4\pi}\int_{S_i}[\nabla G_i(\mathbf{r}-\mathbf{r}')E_i(\mathbf{r}') - m_i G_i(\mathbf{r}-\mathbf{r}')\nabla E_i(\mathbf{r}')]\mathrm{d}\mathbf{S}' \qquad \mathbf{r}\in V_i, \tag{5}$$

n denoting the surface normal pointing outwards, the symbols +,− representing the surface integral when considered from outside or inside, respectively, and $G_{0,i}$ is the Green's function in 2D,[35] that is, $G_{0,i}(\mathbf{r}-\mathbf{r}') = \pi i H_0^{(1)}(2\pi\sqrt{\epsilon_{0,i}}|\mathbf{r}-\mathbf{r}'|)$ and $\nabla G_{0,i}(\mathbf{r}-\mathbf{r}') = \pi i\sqrt{\epsilon_{0,i}}H_1^{(1)}(2\pi\sqrt{\epsilon_{0,i}}|\mathbf{r}-\mathbf{r}'|)$, where $H_{0,1}^{(1)}$ are the zeroth- and first-order Hankel functions of the first kind, respectively. In the *s* polarization mode $m = 1$, whereas for *p* polarization $m_i = \sqrt{\epsilon_0}/\sqrt{\epsilon_i}$. To obtain Eq. (5) we have made use of the boundary conditions $E_i^+(\mathbf{r})|_{\mathbf{r}\in S_i} = E_i^-(\mathbf{r})|_{\mathbf{r}\in S_i}$ and $m_i\mathbf{n}\nabla E_i^+(\mathbf{r})|_{\mathbf{r}\in S_i} = \mathbf{n}\nabla E_i^-(\mathbf{r})|_{\mathbf{r}\in S_i}$, where the superscripts +,− denote the field taken from the outside or the inside of volume V_i, respectively. Equations (4) and (5) can be solved numerically to any degree of accuracy by discretizing the surfaces S_i and solving the coupled equations through matrix inversion. This method is well known in scattering from random rough surfaces[31–33,36,37] and has been implemented in the study of interactions between particles and substrates,[27,28,38] so it will not be described here. A detailed implementation of the method is presented in Ref. 32. A comparison of the different methods for solving the scattering equations can be found in Ref. 39. One of the main advantages of the method employed here is that all resonances (surface and bulk) are accurately obtained without need of high sampling. This is one of the main drawbacks of finite-difference-time-domain methods, since in the presence of resonances it is well known that the number of elements must be increased considerably.[39]

Once the boundary values E_i and ∇E_i have been obtained the scattered intensity is well defined for all values of **r** through Eq. (4). Considering a plane wave as an incident pump intensity, we define the scattering cross section of the collection of M 2-D objects of average radius R in the far field as[40]

$$C_{\mathrm{sc}} = \frac{1}{M}\frac{\lambda}{2\pi R}\frac{1}{\pi}\int_0^{2\pi}\frac{|E(r,\theta)|^2}{P_{\mathrm{inc}}}r\mathrm{d}\theta \qquad r\gg\lambda, \tag{6}$$

where E is given by Eq. (4), and P_{inc} is the average power incident on the system. In the limit where there is no interaction between the objects $C_{\mathrm{sc}} = \Sigma_{i=1}^{M}C_{\mathrm{sc}}^i/M$, where C_{sc}^i is the scattering cross section of object i isolated. (When all objects have the same geometry and orientation, $C_{\mathrm{sc}} = C_{\mathrm{sc}}^1$). We wish to emphasize that even though in the following we consider only cylindrical scatterers because of their high Q factor, Eqs. (4) and (5) can be applied to any collection of scatterers with arbitrary geometry and orientation. In this work we have defined the Q factor as

$$Q = \frac{\Delta\omega_{\mathrm{res}}}{\omega_{\mathrm{res}}}, \tag{7}$$

where ω_{res} is the resonance frequency and $\Delta\omega_{\mathrm{res}}$ is the FWHM of the resonance in hertz.

3. RESULTS AND DISCUSSION

A. Results with a Single Cylinder

The parameters used for Eqs. (1) and (2) are shown in Table 1, where the center wavelength for the laser transition is $\lambda_{\mathrm{laser}} = 500$ nm, with FWHM of ≈12 nm. To maintain our findings as general as possible we shall study the resonances for the following cylinder radii: $R = 125$, 250, 500, 750, 1000, and 1500 nm, corresponding to $R = \lambda_{\mathrm{laser}}/4$, $R = \lambda_{\mathrm{laser}}/2$, $R = \lambda_{\mathrm{laser}}$, $R = 3/2\lambda_{\mathrm{laser}}$, $R = 2\lambda_{\mathrm{laser}}$, and $R = 3\lambda_{\mathrm{laser}}$, respectively, and in the wavelength range $\lambda = 460$–540 nm. As mentioned before, gain is introduced through the variation of the average population inversion ΔN_{01}. We will consider all possible values of N_1/N_t from 0% to 100% even though the 100% case corresponds to the limit $|E_{\mathrm{pump}}| \to \infty$.

Results for the isolated case are shown in Fig. 2. The case with $R = 125$ nm ($R = \lambda_{\mathrm{laser}}/4$) is represented in Fig. 2(a) where, for the small particle size, we find a Rayleigh scatterering behavior[40] and, since no resonances are present, only a relatively small increase in C_{sc} due to gain is found. From results obtained for a collection of many $R = 125$-nm particles (results not shown) we have found that C_{sc} increases proportionally with the number of particles, and thus, in the limit of a large number of particles, we predict that results similar to those shown in Ref. 25 would be obtained, in which the scatterers act as point dipoles. By using Rayleigh scatterers with gain we do not expect a significant increase in the Q factor, whatever the distance between them (we recall that the scattering coefficient μ_s changes as $\mu_s = \rho C_{\mathrm{sc}}^1$, where ρ is the particle density[40,41]).

More interesting results are found for the $R = 250$-nm ($R = \lambda_{\mathrm{laser}}/2$) case shown in Fig. 2(b), since for this particle size there is a single resonance present in the $\lambda = 460$–540-nm range. The modulus of the scattered intensity for this particle radius is shown in Fig. 3 for the $N_1/N_t = 50\%$ and 90% cases. This resonance corresponds to the $(n, \ell) = (5, 1)$ Mie resonance in *s* po-

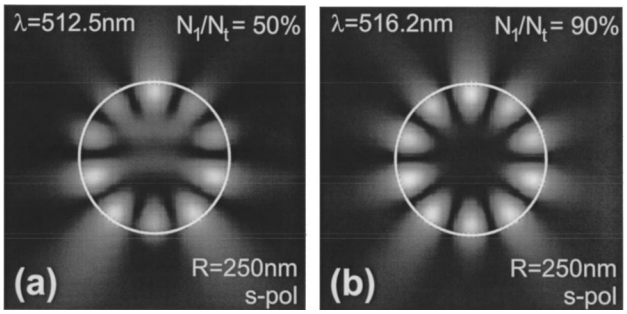

Fig. 3. Modulus of the scattered electric field for *s* polarization for the $R = 250$-nm case presented in Fig. 2(b) for $N_1/N_t =$ (a) 50%, (b) 90%, corresponding to wavelengths $\lambda = 512.5$ nm [Mie resonance $(n, \ell) = (5, 1)$ for $n_1 = 2.4$] and $\lambda = 516.2$ nm, respectively. White indicates stronger electric field values.

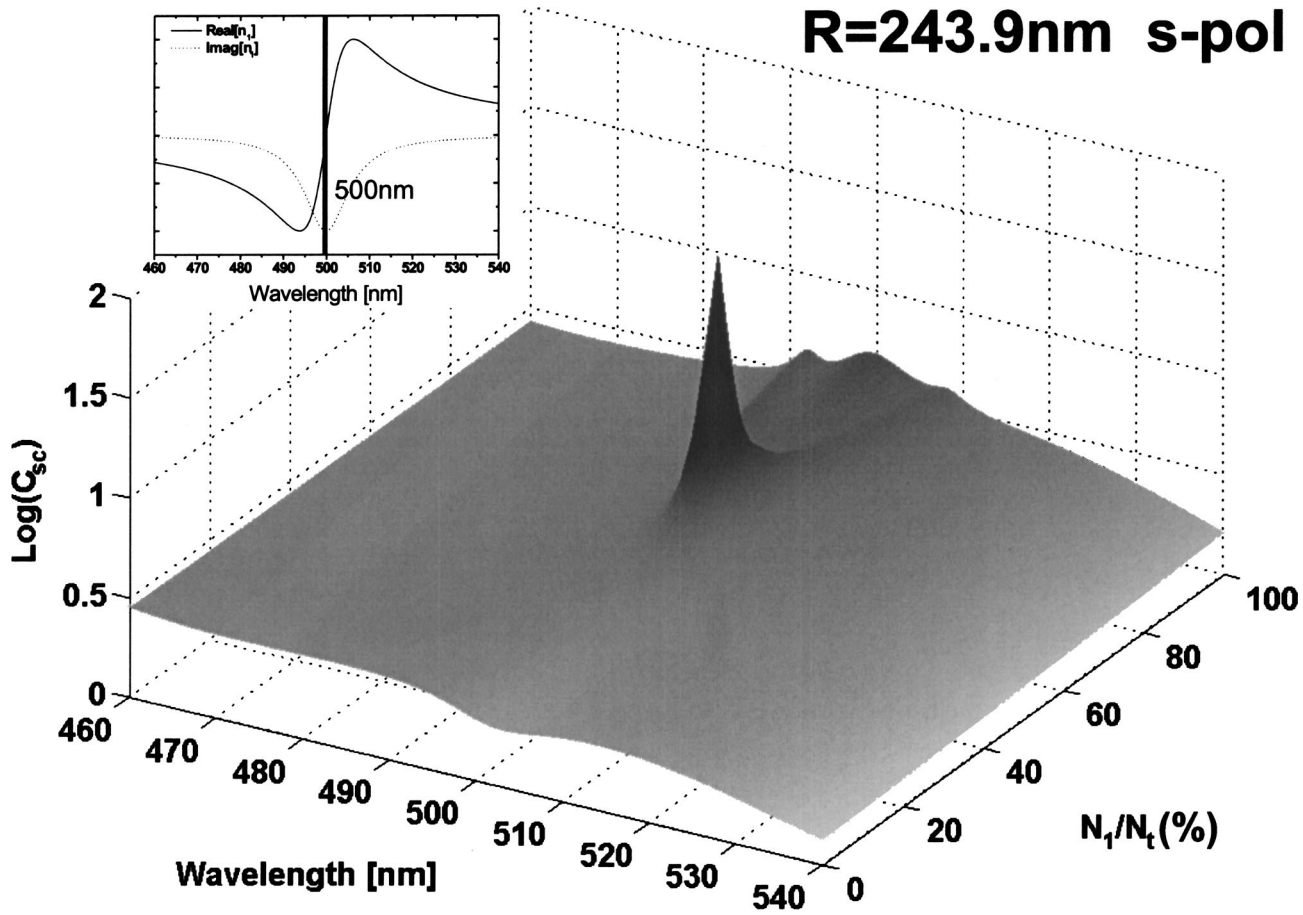

Fig. 4. Scattering cross section in log–scale for a single cylinder for s polarization versus N_1/N_t and λ for an optimized radius $R = 243.9$ nm for which the Mie resonance $(n, \ell) = (5, 1)$ is located at the maximum gain wavelength $\lambda = 500$ nm. The inset shows a normalized value of the real and imaginary parts of the index of refraction for comparison and indicates the location of the $(n, \ell) = (5, 1)$ resonance.

larization for cylinders and is located at $\lambda = 512$ nm (corresponding to size $x = 2\pi R/\lambda$ of $x = 1.5325$ for $n = 2.4$). This is a morphology-dependent resonance[27] for which the principal mode number $n = 5$ indicates the order of the Bessel and Hankel functions describing the partial-wave radial field distribution, and the order $\ell = 1$ indicates the number of maxima in the radial dependence of the internal field distribution. It is well known that cavity Q increases as n increases and as ℓ decreases, and that for a given R, the $\ell = 1$ modes have the highest theoretical Q.[42] The most important features of Fig. 2(b) for this particle size with the optical properties shown in Fig. 1 are (a) that the resonance is maintained and increases with the pump intensity (similar results were found in Ref. 22 for the one-dimensional case), (b) the increase in C_{sc} is nonlinear, and (c) no other resonances appear in the wavelength range 460–540 nm, which means a high free spectral range. The case $R = 250$ nm will be studied in more detail below. Similar results were obtained for the $R = 500$-nm case ($R = \lambda_{laser}$), where we found, however, a shorter free spectral range.

Figures 2(d), (e), and (f) show the cases for $R = 750$, 1000, and 1500 nm, respectively. All these particle sizes have the following feature in common: Since their larger sizes lead to the appearance of multiple resonances, slight changes in the index of refraction influence considerably

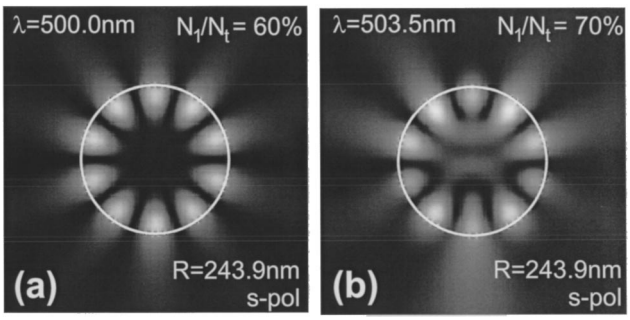

Fig. 5. Modulus of the scattered electric field for s polarization for the $R = 243.9$-nm case presented in Fig. 4 for N_1/N_t = (a) 60%, (b) 70% corresponding to wavelengths $\lambda = 500.0$ nm and $\lambda = 503.5$ nm, respectively. Note how a very small change in N_1/N_t causes a dramatic change in the resonance. White indicates stronger electric field values.

the resonance spectrum. We see that changes in the population inversion induce changes in the complex index of refraction (see Fig. 1) and the modes are not maintained. Therefore, even though some of these modes have higher Q factors than for the $R = 250$-nm and $R = 500$-nm cases [Figs. 2(b) and (c)] as a result of higher principal mode numbers n, the free spectral range will not only be shorter than in the $R = 250$-nm case, but we ex-

pect that as the pumping intensity increases the lasing peaks will appear at different wavelengths, thus inhibiting a stable lasing mode.

Based on the results inferred from Fig. 2, we will now concentrate on the $R = 250$-nm case for the resonance shown in Fig. 3. We shall now study if it is possible to enhance the Q factor of the $(n, \ell) = (5, 1)$ resonance by changing the particle radius so that the resonance maximum falls on the maximum gain value $\lambda = \lambda_{\text{laser}} = 500\,\text{nm}$ (see Fig. 1), which corresponds to $R = 243.9\,\text{nm}$. Results similar to those of Fig. 2(b) are shown in Fig. 4, where we see that the scattering cross section increases, but that the resonance is not maintained for $N_1/N_t > 65\%$ (the inset of Fig. 4 shows where the resonance maximum falls with respect to the real and imaginary values of the index of refraction). This result was not anticipated, since one expects that higher C_{sc} values would be obtained when gain is increased. The reason for this sharp drop in the scattering cross section may be understood in terms of the Mie coefficients.[40] It is well known that the sharpest Mie resonances are found for poles of the Mie coefficients lying closest to the real axis.[43,44] Through numerical analysis performed by changing the real and imaginary parts of n_1 for $R = 243.9\,\text{nm}$ and $\lambda = \lambda_{\text{laser}} = 500\,\text{nm}$, we found that the sharpest peak for the Mie coefficients for $n = 5$ is located at a complex index of refraction $n_1 = n_{\text{opt}} = 2.4105 - 0.0115i$. Therefore, as gain increases, n_1 approaches this value (see Fig. 1) until an optimum gain at which $|n_1 - n_{\text{opt}}|$ is minimum. Further increase of the gain leads to increases in $|n_1 - n_{\text{opt}}|$, therefore making the peak smaller and less sharp. In Fig. 2(b) we see that this n_{opt} value is reached for $R = 250\,\text{nm}$ at $N_1/N_t = 90\%$, and that it is surpassed for $R = 243.9\,\text{nm}$ in Fig. 4 at $N_1/N_t > 65\%$. The form of the amplitude of the scattered field at the resonance and immediately after is shown in Fig. 5, where it is clearly seen that at $N_1/N_t = 70\%$ the sharp resonance is lost and a new resonance with much smaller Q is formed. Results similar to those shown in Figs. 4 and 5 were obtained when tuning the resonance at different positions that were equivalent to placing the maximum C_{sc} shown in Fig. 4 at different N_1/N_t values. The results for $R = 250\,\text{nm}$ correspond to a shifting of this maximum to the $N_1/N_t = 95\%$ position. From these results it is clear that by selectively changing the size within a very small range, we may tune the resonance to $\lambda = \lambda_{\text{laser}}$, thus lowering the threshold considerably. However, if we surpass a certain pump intensity, this high Q factor will be lost abruptly. If stable lasing modes for a large range of pumping intensities are desired, then the instance shown in Fig. 2(b) in which the resonance maximum does not coincide with λ_{laser} is the most appropriate. If lasing modes with higher Q and lower threshold are desired, then the instance shown in Fig. 4 where the resonance maximum coincides with λ_{laser} is the most appropriate; however, this high Q factor will

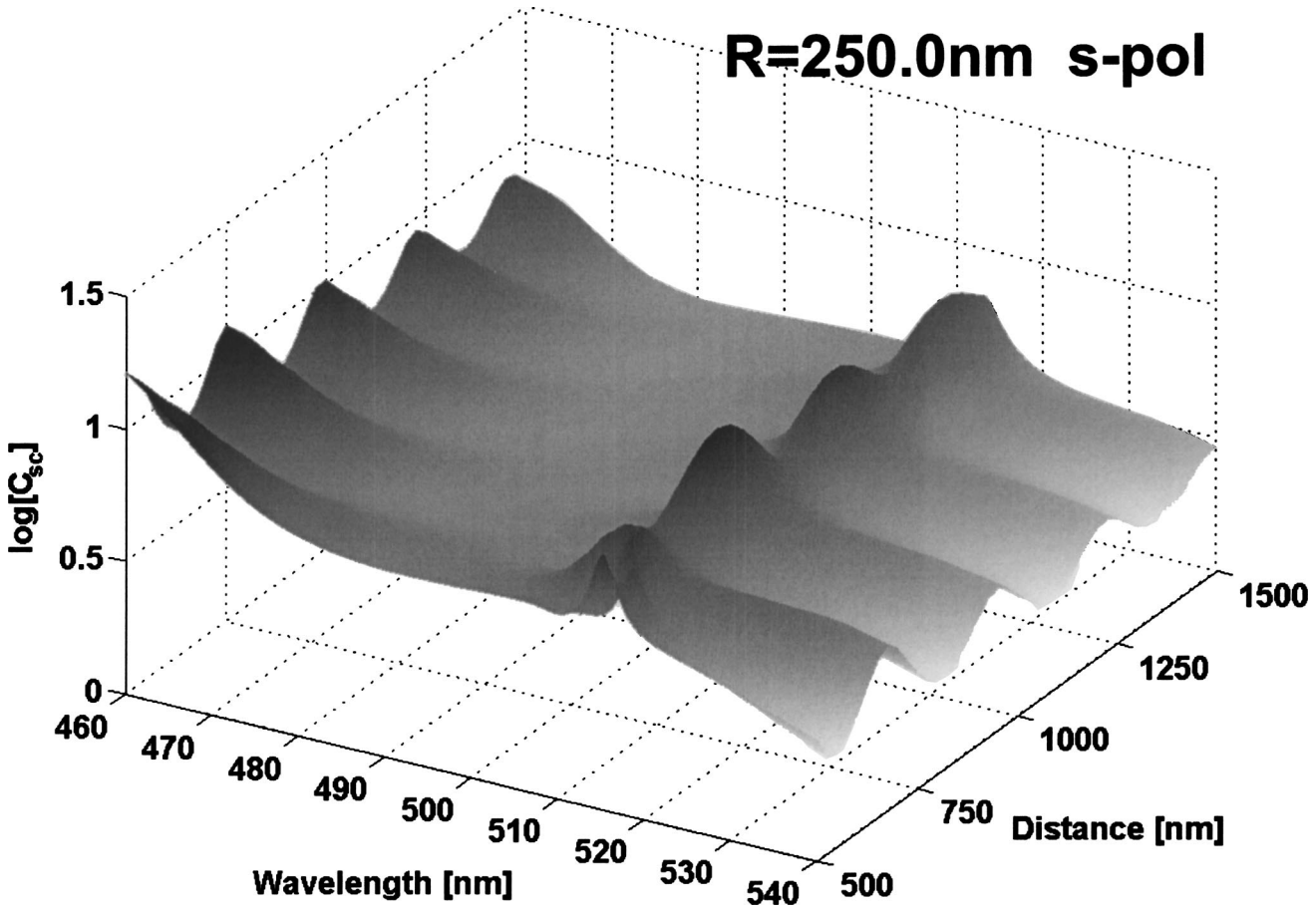

Fig. 6. Scattering cross section in log–scale for two cylinders of $R = 250\,\text{nm}$ and $N_1/N_t = 50\%$ for s polarization versus λ and the distance between their centers d in nanometers.

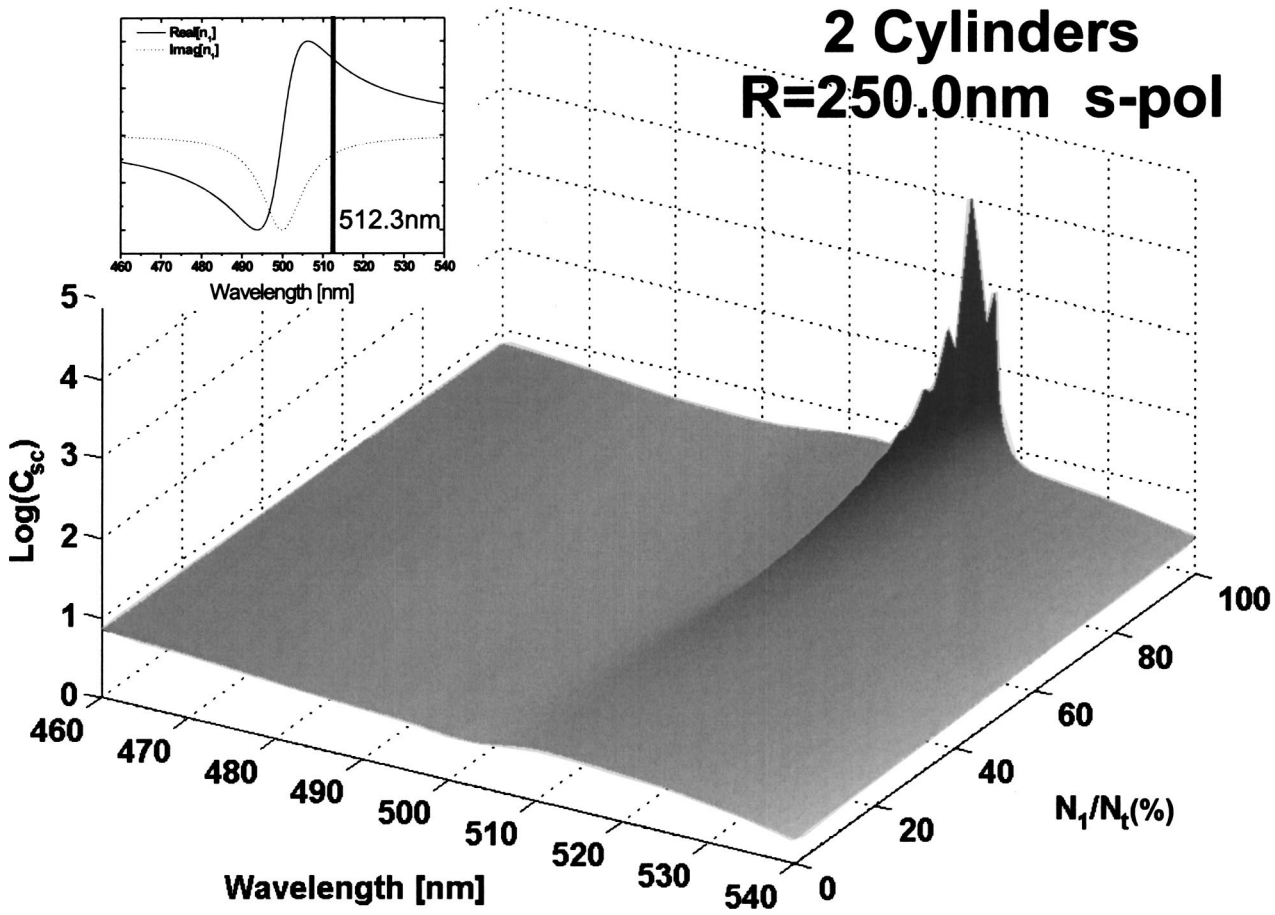

Fig. 7. Scattering cross section in log–scale for two cylinders of $R = 250\,\text{nm}$ separated by $d = 850\,\text{nm}$ (see Fig. 6) for s polarization versus N_1/N_t. The inset shows a normalized value of the real and imaginary parts of the index of refraction for comparison and indicates the location of the $(n, \ell) = (5, 1)$ resonance.

be lost at high pump intensities. This in fact can be used to create a Q switching mode, since we expect that pumping intensities that create a population difference that places the system close to the maximum value of the resonance will create an unstable situation in which the maximum Q factor will be reached and lost cyclically.

B. Results with Multiple Cylinders

Once we have studied the optimization of a particular resonance for an isolated cylinder, the following questions are investigated: Can the high Q of this optimized resonance be increased further in the presence of additional particles? What configuration of particles produces the maximum result? We have studied the $R = 250$-nm case shown in Fig. 2(b) for two and three cylinders, maintaining a constant separation between their centers (in the three-cylinder case the axes of the cylinders were at the vertices of an isosceles triangle). The change in the scattering cross section for two cylinders at a separation d between their centers is shown in Fig. 6 for the $N_1/N_t = 50\%$ case (no gain or absorption). As expected, a sinusoidal pattern is seen as the separation d increases corresponding to constructive and destructive interference. Since a maximum in C_{sc} is found for $d = 850\,\text{nm}$, we have maintained this distance and introduced gain in both cylinders, as was done before. Results for this configuration are shown in Fig. 7, where we find a very strong increase in C_{sc} as compared with Fig. 2(b) of four orders of magnitude. The amplitude of the scattered field for the $N_1/N_t = 90\%$ case is shown in Fig. 8, where we see that this high C_{sc} arises as a result of the development of a collective resonance. We see that the same resonance shown in Figs. 3(b) and 5(a) appears at both cylinders simultaneously. The minima found in Fig. 6 correspond to the case when the resonance is fully excited in only one of the scatterers. Obviously, such high-Q resonances as those shown in Fig. 7 will be practically impossible to obtain experimentally because of surface de-

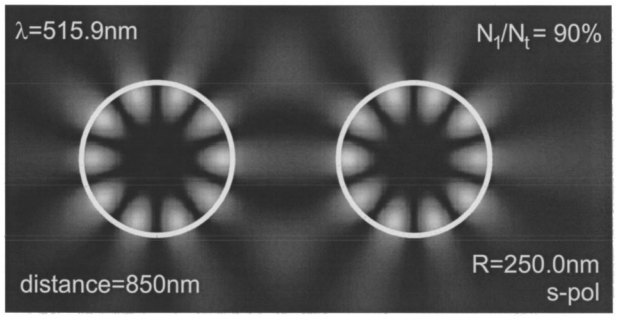

Fig. 8. Modulus of the scattered electric field for s polarization for two cylinders of $R = 250\,\text{nm}$ separated $d = 850\,\text{nm}$ for the $N_1/N_t = 90\%$ case presented in Fig. 7 corresponding to $\lambda = 515.9\,\text{nm}$.

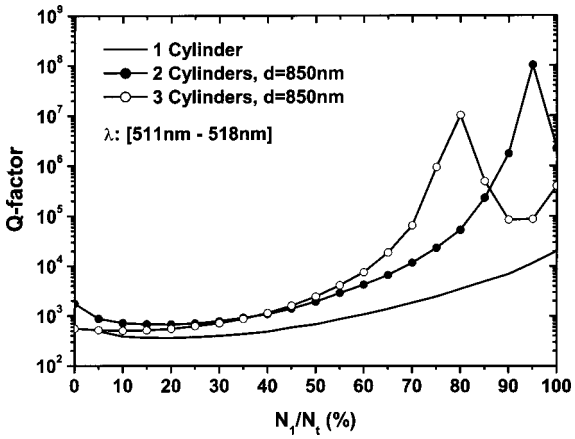

Fig. 9. Q factor ($\Delta\omega/\omega$ of the resonance peak) for a single cylinder of $R = 250$ nm, solid curve; two cylinders of $R = 250$ nm separated $d = 850$ nm, filled circles; three cylinders of $R = 250$ nm separated $d = 850$ nm, open circles.

fects, since high symmetries are needed. However, it is clear from Figs. 6 and 7 that the presence of a second particle increases the scattering cross section nonlinearly when collective resonances are excited, i.e., when the configuration is optimized. Also, from Fig. 6 we infer that the collective resonance does not have a sharp peak at a certain separation, but that it is maintained for a range of over 50 nm. Similar results were obtained for three cylinders, where the optimum separation was again in the vicinity of $d = 850$ nm.

The increase in Q factor when a collective resonance is excited is more clearly shown in Fig. 9 for the isolated cylinder, two cylinders, and three cylinders at a separation $d = 850$ nm for $R = 250$ nm. From this figure we see that there is an increase of four orders of magnitude of the Q factor when comparing the isolated cylinder with the two-cylinder case. We see that the addition of a third cylinder does not help in increasing the Q factor but considerably lowers the threshold. We once again see a decay of the Q factor as we increase gain above a certain value for the same reasons presented in Subsection 3.A. We would like to point out that these results were obtained for a resonance with high free spectral range [see Fig. 2(b)]. As we increase the size of the cylinders (see Fig. 2), the decrease in the free spectral range will result in a decrease of the Q factor. Also as mentioned in Subsection 3.A, for larger radii we expect that as the pumping intensity increases, the lasing peaks will appear at different wavelengths, thus inhibiting a stable lasing mode.

4. CONCLUSIONS

We have presented results for the scattering cross section of one, two, and three cylinders with gain versus wavelength and population inversion. From the work presented here, the following main conclusions may be drawn:

1. The optimal size for a stable, cylindrical, microcavity laser is such that a very few well-separated resonances are excited within the lasing FWHM.
2. By selectively tuning the position of the resonance maximum through changes in the radius, it is possible to lower the threshold.
3. Depending on the resonance, it is possible that after a certain gain, the Q factor decreases, raising the prospect of Q switched microcavities.
4. The presence of a second identical scatterer increases the Q factor nonlinearly; in the cases presented here we have shown an increase of four orders of magnitude when a collective mode is excited at certain optimized separations.
5. This increase in the Q factor does not continue as additional particles are included; however, the threshold is found to decrease.

Even though the results presented here are for a small number of particles, we anticipate that important conclusions may be reached for the development of high-Q-factor and low-threshold random lasers. In particular, scatterers with gain of small size ($R < \lambda_{\text{laser}}/4$) will not produce high-$Q$ lasing. Also, we predict that high Q factors and low threshold values will be obtained when the average distance between particles is optimized so that collective particle resonances may be excited for particle sizes in the range of $\lambda_{\text{laser}}/2 \leqslant R \leqslant \lambda_{\text{laser}}$. Additionally, if large particle sizes are used ($R > \lambda_{\text{laser}}$), we expect that there will be an overlap of the lasing modes, and the emission will be continuous. On the other hand, if small particles in the range $\lambda_{\text{laser}}/2 \leqslant R \leqslant \lambda_{\text{laser}}$, or small overall system sizes of the order of a few λ_{laser} are used, discrete lasing peaks will be observed as reported in Ref. 17.

ACKNOWLEDGMENTS

J. Ripoll acknowledges support from European Union project FMRX-CT96-0042.

Corresponding author J. Ripoll may be reached by e-mail to jripoll@iesl.forth.gr.

REFERENCES

1. A. E. Siegman, *Lasers* (University Science, Mill Valley, Calif., 1986).
2. E. Wolf, ed., *Progress in Optics, Vol. XLI* (Elsevier North-Holland, Amsterdam, 2000).
3. R. E. Benner, P. W. Barber, J. F. Owen, and R. K. Chang, "Observation of structure resonances in the fluorescence spectra from microspheres," Phys. Rev. Lett. **44**, 475–477 (1980).
4. H.-B. Lin, J. D. Eversole, and A. J. Campillo, "Spectral properties of lasing microdroplets," J. Opt. Soc. Am. B **9**, 43–50 (1992).
5. D. W. Vernooy, V. S. Ilchenko, H. Mabuchi, E. W. Streed, and H. J. Kimble, "High-Q measurements of fused-silica microspheres in the near infrared," Opt. Lett. **23**, 247–249 (1998).
6. V. Sandoghdar, F. Treussart, J. Hare, V. Lefevre-Seguin, J.-M. Raimond, and S. Haroche, "Very low threshold whispering-gallery-mode microsphere laser," Phys. Rev. A **54**, R1777–R1780 (1996).
7. J. F. Owen, P. W. Barber, P. B. Dorain, and R. K. Chang, "Enhancement of fluorescence induced by microstructure resonances of a dielectric fiber," Phys. Rev. Lett. **47**, 1075–1078 (1981).

8. H.-J. Moon, Y.-T. Chough, and K. An, "Cylindrical microcavity laser based on the evanescent-wave-coupled gain," Phys. Rev. Lett. **85**, 3161–3614 (2000).
9. D. S. Weiss, V. Sandoghdar, J. Hare, V. Lefevre-Seguin, J.-M. Raimond, and S. Haroche, "Splitting of high-*Q* Mie modes induced by light backscattering in silica microspheres," Opt. Lett. **20**, 1835–1837 (1995).
10. P. M. Visser, K. Allart, and D. Lenstra, "Dielectric structures with bound modes for microcavity lasers," Phys. Rev. E **65**, 056604 (2002).
11. V. S. Letokhov, "Generation of light by a scattering medium with negative resonance absorption," Sov. Phys. JETP **26**, 835–840 (1968).
12. N. M. Lawandy, R. M. Balachandran, A. S. L. Gomes, and E. Sauvain, "Laser action in strongly scattering media," Nature **368**, 436–438 (1994).
13. M. Siddique, R. R. Alfano, G. A. Berger, M. Kempe, and A. Z. Genack, "Time-resolved studies of stimulated emission from colloidal dye solutions," Opt. Lett. **21**, 450–452 (1996).
14. S. John, "Localization of light," Phys. Today **44**, 32–40 (1991).
15. D. S. Wiersma, "Light diffusion with gain and random lasers," Phys. Rev. E **54**, 4256–4265 (1996).
16. H. Cao, Y. G. Zhao, H. C. Ong, S. T. Ho, J. Y. Dai, J. Y. Wu, and R. P. H. Chang, "Ultraviolet lasing in resonators formed by scattering in semiconductor polycrystalline films," Appl. Phys. Lett. **73**, 3656–3658 (1998).
17. H. Cao, Y. G. Zhao, S. T. Ho, E. W. Seelig, Q. H. Wang, and R. P. H. Chang, "Random laser action in semiconductor powder," Phys. Rev. Lett. **82**, 2278–2281 (1999).
18. H. Cao, J. Y. Xu, S.-H. Chang, and S. T. Ho, "Transition from amplified spontaneous emission to laser action in strongly scattering media," Phys. Rev. E **61**, 1985–1989 (2000).
19. S. V. Frolov, Z. V. Vardeny, A. A. Zakhidov, and R. H. Baughman, "Laser-like emission in opal photonic crystals," Opt. Commun. **162**, 241–246 (1999).
20. Y. Ling, H. Cao, A. L. Burin, M. A. Ratner, X. Liu, and R. P. H. Chang, "Investigation of random lasers with resonant feedback," Phys. Rev. A **64**, 063808 (2001).
21. G. Zacharakis, N. Papadogiannis, G. Filippidis, and T. G. Papazoglou, "Photon statistics of laserlike emission from polymeric scattering gain media," Opt. Lett. **25**, 923–925 (2000).
22. X. Jiang and C. M. Soukoulis, "Time-dependent theory for random lasers," Phys. Rev. Lett. **85**, 70–73 (2000).
23. C. Vanneste and P. Sebbah, "Selective excitation of localized modes in active random media," Phys. Rev. Lett. **87**, 183903 (2001).
24. Q. Li, K. M. Ho, and C. M. Soukoulis, "Mode distribution in coherently amplifying random media," Physica B **296**, 78–84 (2000).
25. A. L. Burin, M. A. Ratner, H. Cao, and R. P. H. Chang, "Model for a random laser," Phys. Rev. Lett. **87**, 215503 (2001).
26. S. John and G. Pang, "Theory of lasing in a multiple-scattering medium," Phys. Rev. A **54**, 3642–3652 (1996).
27. J. R. Arias-Gonzalez and M. Nieto-Vesperinas, "Near-field distributions of resonant modes in small dielectric objects on flat surfaces," Opt. Lett. **25**, 782–784 (2000).
28. J. R. Arias-Gonzalez and M. Nieto-Vesperinas, "Radiation pressure over dielectric and metallic nanocylinders on surfaces: polarization dependence and plasmon resonance conditions," Opt. Lett. **27**, 2149–2151 (2002).
29. M. Lester, J. R. Arias-Gonzalez, and M. Nieto-Vesperinas, "Fundamentals and model of photonic-force microscopy," Opt. Lett. **26**, 707–709 (2001).
30. J. R. Arias-Gonzalez, M. Nieto-Vesperinas, and M. Lester, "Modeling photonic-force microscopy with metallic particles under plasmon eigenmode excitation," Phys. Rev. B **65**, 115402 (2002).
31. J. M. Soto-Crespo and M. Nieto-Vesperinas, "Scattering from very rough random surfaces and deep reflection gratings," J. Opt. Soc. Am. A **6**, 367–384 (1989).
32. A. A. Maradudin, T. Michel, A. R. McGurn, and E. R. Mendez, "Enhanced backscattering of light from a random grating," Ann. Phys. (N.Y.) **203**, 255–307 (1990).
33. M. Nieto-Vesperinas, *Scattering and Diffraction in Physical Optics* (Pergamon, New York, 1996).
34. Z. Chen, A. Taflove, and V. Backman, "Equivalent volume-averaged light scattering behavior of randomly inhomogeneous dielectric spheres in the resonant range," Opt. Lett. **28**, 765–767 (2003).
35. G. B. Arfken and H. J. Weber, *Mathematical Methods for Physicists* (Academic, New York, 1995).
36. J. A. Ogilvy, *Theory of Wave Scattering from Random Rough Surfaces* (Adam Hilger, Bristol, 1991).
37. J. A. Sanchez-Gil and M. Nieto-Vesperinas, "Light scattering from random rough dielectric surfaces," J. Opt. Soc. Am. A **8**, 1270–1286 (1991).
38. J. Ripoll, A. Madrazo, and M. Nieto-Vesperinas, "Scattering of electromagnetic waves from a body over a random rough surface," Opt. Commun. **142**, 173–178 (1997).
39. T. Wriedt and U. Comberg, "Comparison of computational scattering methods," J. Quant. Spectrosc. Radiat. Transf. **60**, 411–423 (1998).
40. H. C. van de Hulst, *Light Scattering by Small Particles* (Dover, New York, 1981).
41. A. Ishimaru, *Wave Propagation and Scattering in Random Media* (Academic, New York, 1978).
42. H.-B. Lin, A. L. Huston, J. D. Eversole, and A. J. Campillo, "Internal scattering effects on microdroplet resonant emission structure," Opt. Lett. **17**, 970–972 (1992).
43. P. R. Conwell, P. W. Barber, and C. K. Rushforth, "Resonant spectra of dielectric spheres," J. Opt. Soc. Am. A **1**, 62–67 (1984).
44. B. A. Hunter, M. A. Box, and B. Maier, "Resonance structure in weakly absorbing spheres," J. Opt. Soc. Am. A **5**, 1281–1286 (1988).